Diagnosing the Topside Ionosphere Using Synchronous E- and B-field Measurements from the Swarm Satellite Constellation

Ivan P. Pakhotin[1], Ian Robert Mann[1], David Knudsen[2], Johnathan K Burchill[2], Louis Ozeke[1] , Jesper W Gjerloev[3], Jonathan I Rae[4], Colin Forsyth[4] , Kyle Murphy[5], Georgios Balasis[6] and Ioannis A. Daglis[7]

(1) University of Alberta, Department of Physics, Edmonton, AB, Canada
(2) University of Calgary, Calgary, AB, Canada
(3) Johns Hopkins University Applied Physics Laboratory, Laurel, MD, United States
(4) University College London, London, United Kingdom
(5) NASA Goddard Space Flight Center, Greenbelt, MD, United States
(6) National Observatory of Athens, Athens, Greece
(7) National and Kapodistrian University of Athens, Athens, Greece

Abstract

This study explores the potential for using the synchronous E-field and B-field measurements from the Swarm satellite constellation for diagnosing the topside ionosphere. Within the framework of reflected and interfering Alfven waves interacting with a reflecting boundary, we examine the use of the spectral properties of these fields to infer key local ionospheric parameters such as Pedersen conductivity, Alfven speed and distance from the reflective layer. These techniques have the potential to present more accurate estimates of the potential dynamical and spatial variation of these important quantities than relying on empirical or statistical models such as International Reference Ionosphere.

Introduction

• Electromagnetic waves travelling through plasma have characteristics which are governed by the medium through which they are travelling. This presents opportunities to use wave parameters to infer key plasma properties

• One example is the use of the harmonics of the ionospheric Alfven resonator (IAR) to determine the F-region density (Parent et al., 2010). This was corroborated through independent measurements from the collocated Digisonde, riometer and all-sky imager at HAARP

• Swarm is a multi-spacecraft ESA mission launched in 2013 into low-Earth polar orbit at ~450 km altitude for Swarm A and C and ~550 km altitude for Swarm B. The spacecraft carry 50 Hz fluxgate magnetometers and 16 Hz electric field measurement instruments. The spacecraft also have a 16 Hz Langmuir probe for measuring plasma density from electric potential

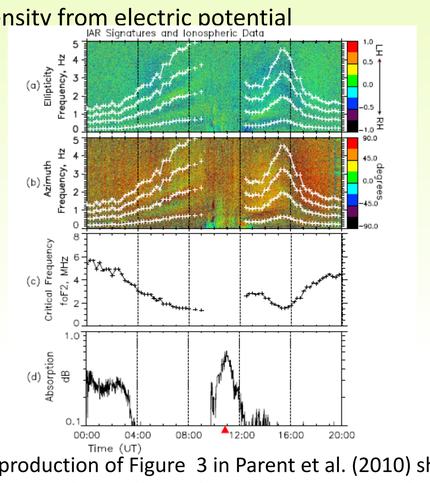

Figure 1: reproduction of Figure 3 in Parent et al. (2010) showing (a, b) IAR measurements on Gakona induction magnetometer on 28 February 2006, overplotted with predicted model IAR frequencies (in white) driven by the f0F2 measurements from the HAARP Digisonde (c). Note the correspondence between the model and IAR harmonic observations. (d) shows riometer absorption at HAARP.

• This study presents the framework for inferring parameters such as height-integrated Pedersen conductivity, effective Alfven speed and ion mass ratio, as well as preliminary results

Methodology

• The diagram in Figure 2 shows a simple case of plane wave reflection from a reflecting boundary. It can be seen that a quasi-stationary interference pattern forms near the boundary due to the wave's mutual interference. This is true for both a single reflection from the ionospheric boundary and for a dual reflection from the ionospheric boundary and from the Alfven speed gradient above the

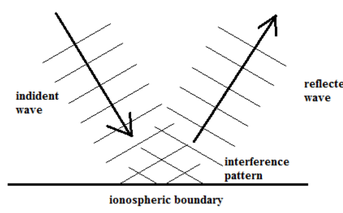

Figure 2: a schematic of a reflecting plane wave. An interference pattern forms near the ionospheric reflecting boundary.

• Figure 3 shows the model of single reflection outlined in Knudsen et al. (1992). It can be seen that the impedance (top) and E-B phase difference (bottom) are periodic as a function of frequency, with impedance oscillating between Zp (Pedersen impedance) and Za^2Σp where Za = μ0Va is the Alfven impedance. Thus observing these 2 limits will make it possible to measure both Pedersen conductance and effective Alfven speed. The periodicity is dependent on distance of the observer from the boundary.

Wave interference models

Meanwhile Figure 4 shows the modelled IAR case (Lysak et al., 1991). A similar pattern can be observed here with impedance and phase both varying periodically with frequency between two limits.

In the case of the IAR, there is no dependence of height from the conducting layer, so the phase and impedance functions are observer-independent.

Single reflection

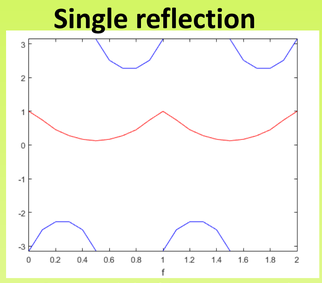

Figure 3: a model of Knudsen et al. (1992) for parameters representative of Figure 5 interval, showing normalised E/B ratio (red) and phase (blue).

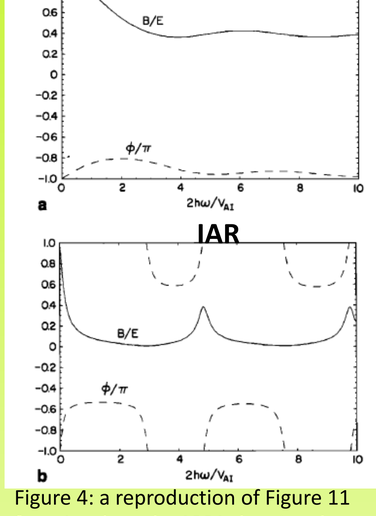

Figure 4: a reproduction of Figure 11 from Lysak et ak., 1991 showing the relative B/E ratio and phase shift for a) weak reflection and b) strong reflection

31st May 2014

• Figure 5 shows cross-track B-field and ion velocity measurements for an auroral crossing period on 31 May 2014. It can be seen that the measurements are coherent across the entire crossing (Figure 5, a) while the frequency-domain plots (Figure 5, b and c) show that they are also self-similar across all frequencies. Note that the cross-track ion velocity corresponds to along-track E-field via E = -v x B so the two measurements are in fact of orthogonal B-field and E-field components.

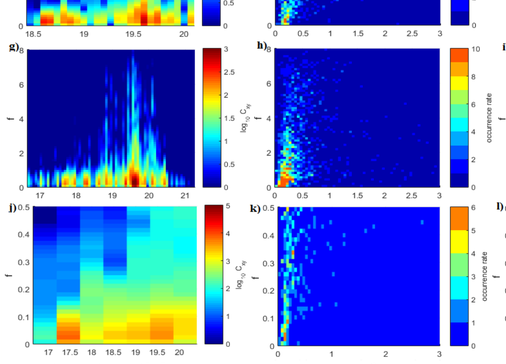

Figure 5: a) time series plot of cross-track B-field (red) and ion velocity (blue) data, b) the FFT of the B-field data, and c) the FFT of the ion velocity data, for the same interval. Bottom: AMPERE plot, blue-Swarm A, red-Swarm C

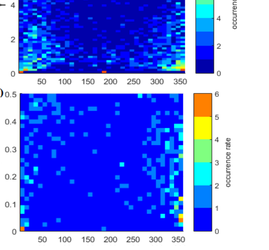

• This coherency can be used to perform histogram analysis on coherent signal, similar to Grzesiak (2000). Figure 6 shows the results for 3 time periods denoted in Figure 5 – Period 1 dominated by low frequencies, Period 2 with significant energy above 1 Hz, and Period 3 which contains the entire auroral crossing including Periods 1 and 2. The bottom 3 panels of Figure 5 show Period 3 with a larger Hanning window applied to resolve the lowest frequencies.

Figure 6: cross power spectral density, impedance and phase histograms for Period 1 (a,b,c) for Period 2 (d,e,f) for Period 3 (g,h,i) and for Period 3 with a larger window focuinsg on low frequencies (j,k,l)

• It can be seen that for all frequencies observed, the lower limit of the impedance histogram (middle) seems to be ~0.12Ω. This is lower than the impedance predicted by the International Reference Ionosphere (IRI) which generates a result of ~0.3 Ω. The discrepancy is believed due to the IRI model not capturing local auroral Σp enhancements during a time of irregular field-aligned currents (FACs). In this way, the technique can be used to validate the global Σp model.

28th August, 2014

• The upper limit does not appear to be as sharp. This is likely due to the fact that the satellite flies perpendicular to field lines and thus the histograms capture an amalgamation of several effective Alfven speeds from several different field lines. This was mentioned in Knudsen et al. (1992) where they note that data from the HILAT satellite is in less agreement with the model than data from the Black Brant X rocket. However, Swarm's high measurement cadence (16 Hz) makes it feasible to take short segments for analysis which may capture effective Alfven speeds more clearly. This is a subject of current work.

• Another time period on 28 August 2014 has been analysed in a similar manner. This time the FAC system from AMPERE (Figure 7) shows a more traditional R1/R2 concentric ring structure. Swarm passes from dayside to nightside.

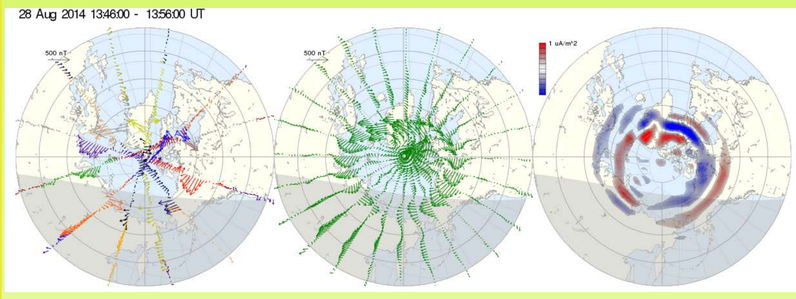

Figure 7: AMPERE raw spacecraft measurements (left), shpherical harmonics fit (middle) and FAC map (right) for 28 August 2014 period. Swarm orbit ~13-01 MLT.

• Dayside histograms are displayed on Figure 8. Nightside FACs are displayed on Figure 9. It can be seen that in both cases there is a cut-off below ~0.2-0.4 Ω which would suggest the Σp limit. Once again there is a diffuse upper limit, making Va calculations difficult. Interestingly, though IRI-derived Σp are much lower on the nightside, the histograms suggest that Σp inside the auroral region are similar. This suggests localised conductivity enhancements, possibly from precipitation.

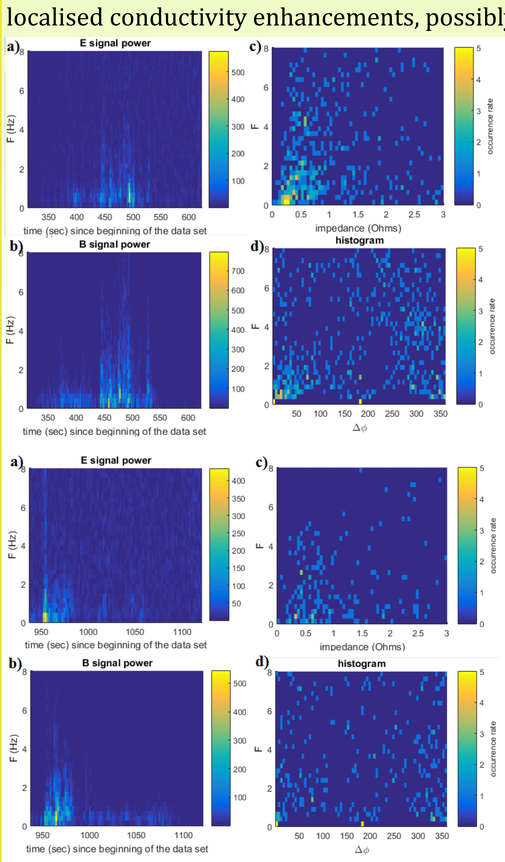

Figure 8: for the dayside auroral crossing, a) cross-track B-field power, b) along-track E-field power, c) impedance and d) phase histograms.

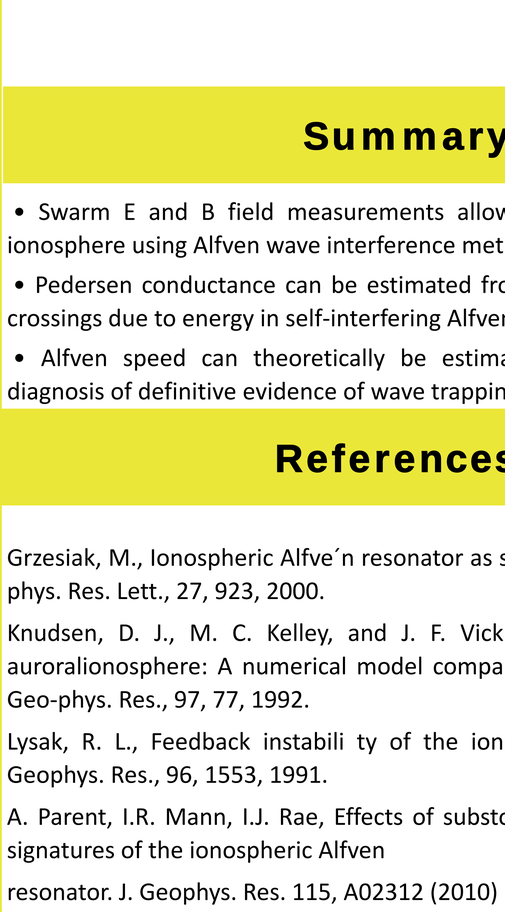

Figure 9: as Figure 8 but for the nightside pass.

Summary

• Swarm E and B field measurements allow diagnosis of the topside ionosphere using Alfven wave interference methods

• Pedersen conductance can be estimated from E/B ratio during auroral crossings due to energy in self-interfering Alfven waves

• Alfven speed can theoretically be estimated, as well as potential diagnosis of definitive evidence of wave trapping in IAR

References

Grzesiak, M., Ionospheric Alfve´n resonator as seen by Freja satellite, Geo-phys. Res. Lett., 27, 923, 2000.

Knudsen, D. J., M. C. Kelley, and J. F. Vickrey, Alfve´n waves in the auroralionosphere: A numerical model compared with measurements, J. Geo-phys. Res., 97, 77, 1992.

Lysak, R. L., Feedback instabili ty of the ionospheric resonant cavity,J. Geophys. Res., 96, 1553, 1991.

A. Parent, I.R. Mann, I.J. Rae, Effects of substorm dynamics on magnetic signatures of the ionospheric Alfven

resonator. J. Geophys. Res. 115, A02312 (2010)

ESA Fourth Swarm Science Meeting

Correspondence: Dr Ivan Pakhotin, pakhotin@ualberta.ca